Spherical microgel colloids — Hard spheres from soft matter

ARTICLE *in* BERICHTE DER BUNSENGESELLSCHAFT/PHYSICAL CHEMISTRY CHEMICAL PHYSICS · NOVEMBER 1998

DOI: 10.1002/bbpc.19981021118

5 AUTHORS, INCLUDING:

Eckhard Bartsch
University of Freiburg
73 PUBLICATIONS **1,719** CITATIONS
SEE PROFILE

Stefan Kirsch
BASF SE
21 PUBLICATIONS **389** CITATIONS
SEE PROFILE

Spherical Microgel-Colloids - Hard Spheres from Soft Matter

E. Bartsch* , S. Kirsch#, P. Lindner§, T. Scherer, S. Stölken
Institut für Physikalische Chemie der Universität Mainz, Jakob-Welder-Weg 15, D-55099 Mainz, Germany
§Institut Laue-Langevin, B.P. 156X, F-38042 Grenoble Cedex, France

Abstract

While gels are usually considered to be soft materials, we demonstrate that is possible to model hard sphere behaviour when the gel structure is confined to spherical objects of sizes in the colloidal range. We have measured the static structure factor of microgel spheres dispersed in good solvents, differing in size, crosslink density and swelling behaviour, by light scattering and small angle neutron scattering. Comparing with theoretical calculations for polydisperse hard spheres we show how the interactions in highly concentrated dispersions of spherical microgel colloids are determined by an interplay of the relative length of dangling polymer ends at the surface (determined by the average crosslink density and the particle size) and the swelling ratio (determined by the average crosslink density and the solvent quality). In addition the swelling ratio controls the volume fraction range in which colloidal behaviour is not superposed by the gel character. The latter leads to a loss of structural order due to the deformablity of the microgel spheres, an effect that occurs at increasingly lower volume fractions if the swelling ratio increases. To achieve hard sphere behaviour up to very high volume fractions, thus, requires high crosslink densities and small swelling ratios.

1. Introduction

The term "gel" usually refers to a macroscopic network of macromolecules or biopolymers due to chemical or physical crosslinking of the chains and typically swollen by a good solvent. It invoques the picture of a soft and yielding material like gelatine. If one limits the extension of the gel to mesoscopic dimensions, i.e. to the colloidal range of several nanometers up to a few microns, by performing the polymerization and chemical crosslinking reactions in microemulsion [1] or by using emulsion polymerization techniques [2], one obtains spherical microgels - entities that are intermediate in behaviour between conventional dispersion colloids and macroscopic gels (cf. Fig.1). Like gels they can be swollen by solvent uptake in a good solvent. However, due to the chemical crosslinking of the polymer chains they retain the spherical shape imparted to them via the synthesis and, thus, their colloidal character. In contrast to conventional colloidal dispersions, e.g. polystyrene latex in water, spherical microgels in a good solvent require no special stabilization to avoid aggregation due to their lyophilic character (negative free enthalpy of mixing).

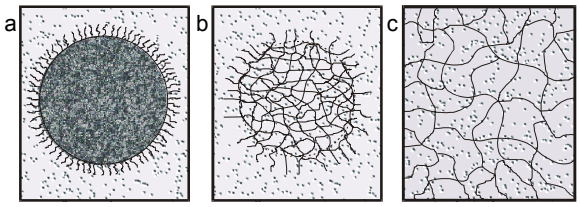

Fig.1 A spherical microgel particle swollen in a good solvent (b) can be considered as an intermediate between a conventional sterically stabilized colloid (a) and a macroscopic polymer gel (c).

Besides technical applications, e.g. for improving the rheological properties of paints in industrial coating processes as well as the performance of films with respect to their weather and shock-resistance [3,4], as "smart fluids" whose behaviour can be controled by external conditions [5,6] or for the development of advanced applications, such as "artificial enzymes", heavy metal scavengers or drug release control [7], microgel colloids have also attracted interest as a model system for fundamental studies on the glass transition problem [8]. Here, profit was made from a well established analogy between atomic fluids and colloidal dispersions [9]. It was shown [8,10] that the dynamics of highly concentrated dispersions of microgel colloids in a good solvent share many features with the slowing down of particle motion observed in dispersions of hard sphere like poly (methylmethacrylate) colloids close to a density driven glass transition [11]. However, significant differences were found in detail [10]. Most strikingly, long time diffusion was not arrested even in the glass state and the glass transition volume fraction φ_g was moved to higher values (0.64 instead of 0.59 for hard spheres). The question has been raised if these findings indicate that the swollen microgel spheres should be considered as rather "soft" spheres (i.e. interacting with a longer ranged soft repulsive potential) and if the mobility of the particles in the glass is due to the higher deformability as compared to hard sphere colloids [10].

In previous work it was demonstrated that the short-range order [12] and the dynamics [13] (and thus the interactions) of microgel particles depend on the average crosslink density. How the crosslink density influences particle interactions is not known in

* To whom all correspondence should be addressed

present address: Polymer Research Laboratory ZKD, BASF Aktiengesellschaft, 67056

detail. It can be surmised that on increasing the crosslink density the volume swelling and, thus, the compressibility of the microgel spheres is reduced. At the same time the chain length of loose polymer ends at the surface which play the same role as the steric stabilization layer in lyophobic colloids is decreased. This means that in the limit of very high crosslink density hard sphere behaviour might be recovered. However, it is not clear which crosslink densities are required and what role is played by the volume swelling as the same nominal crosslink density can yield quite different swelling ratios - depending on the nature of the monomer, the crosslinker and the solvent used [2,14].

In order to better understand the influence of the crosslink density on particle interactions and the properties of concentrated microgel dispersions, we studied the volume fraction dependence of the static structure factor S(q) for three microgel dispersions differing with respect to crosslink density, particle diameter and swelling ratio. The aim was to check if and under which conditions hard sphere behaviour could be achieved and what kind of deviations are to be expected for more weakly crosslinked particles at high concentrations.

2. Experimental

2.1 Microgel Synthesis

Polystyrene (PS) and poly(*t*-butyl acrylate) (PTBA) microgel particles with radii between 25 and 163 nm were synthesized in analogy to Kotera et al. [15] via a batch process of surfactant-free emulsion polymerization using $K_2S_2O_8$ as initiator. In variation of the recipe in Ref.15 a certain amount of crosslinker as comonomer (PS: 1,3 di-iso-propenyl benzene (DIPB); PTBA: ethylenglycol-di-acrylate (EGDA)) was used to form microgel particles. Details of the preparation and purification are described in Ref.2. As particle radii below 90 nm were not accessible in this way, standard emulsion polymerization techniques were used to prepare smaller particle sizes using sodium dodecylsulfate as surfactant and $K_2S_2O_8$ as initiator [16].

2.2 Methods

Light scattering experiments on samples SK-25 and ADM18 (see Tab.1) were performed with an ALV 5000 correlator from ALV, Langen, and a self-made optical set-up [10] with a Ne-YAG solid state ring laser unit (DPSS-50; COHERENT), emitting 50 mW in the TEM_{00} cw mode at a wavelength of λ = 532 nm. For sample ADS257 a standard light scattering equipment (ALV DLS/SLS-5000F) from ALV, Langen, was employed using an argon ion laser (Innova 90-2; from COHERENT) in the TEM_{00} cw mode at a wavelength of λ = 488 nm with a typical power of 100 mW. Small angle neutron experiments (SANS) on sample ADM18 were performed on the instruments PAXE at the Laboratoire Léon Brillouin (LLB) in Saclay (France) and D11 at the Institute Laue-Langevin (ILL) in Grenoble (France) covering q-ranges of $0.02 \le q/nm^{-1} \le 0.46$ and $0.01 \le q/nm^{-1} \le 0.46$, respectively. Further experimental details are given elsewhere [12,16].

table 1 *Results of the particle characterization*

latex	DLS		SLS				
	R_H /nm (aqueous dispersion)	R_H /nm (solvent)	<R>/nm (aqueous dispersion)	<R>/nm (solvent)	S	σ	ΔR/ R_H [%]
SK-25 1:10	163	265	167	270	5-6	0.04§	≈ 1
ADS257 1:50	150	264	-	265	5.5	0.04#	≈ 5
ADM18 1:50	15.3	25	-	-	4.4	0.27*	≈ 50

Particle radii, R_H and <R>, and volume swelling ratio $S = (R_{solv}/R_{aq.disp.})^3$ as determined from light scattering. $R_H = \langle R^6\rangle/\langle R^5\rangle$ denotes the hydrodynamic radius obtained from dynamic light scattering (DLS). <R>, the first moment of the size distribution, was determined by analysing the particle form factor measured by static light scattering (SLS) according to Ref.19. The polydispersity $\sigma = (<R^2>-<R>^2)^{1/2}/<R>$ was obtained by various fractionation techniques. (§ capillary hydrodynamic fractionation; # asymmetric field-flow fractionation; * analytical ultracentrifuge)
Included in the table are the crosslink density (e.g. 1:10 for 10 monomer unit between crosslinks) and the relative ratio ΔR/ R_H of dangling polymer chains at the particle surface with respect to the particle radius. Here it was assumed that the average extension of a dangling end can be equated to the average length of the polymer chains between crosslinks. The latter was approximated by taking 0.25 nm as the length of a monomer unit and multiplying by the number of monomers, as given by the stoichiometric average crosslink density. The used solvents were 4-fluorotoluene for SK-25, 2-ethylnaphthalene for ADS275 as well as fully deuterated toluene for ADM18.

2.3 Sample Characterization

In order to determine the particle size, the intensity autocorrelation function $g^{(2)}(q,\tau)$ [17]

$$g^{(2)}(q,\tau) = \frac{\langle I(q,t)\,I(q,t+\tau)\rangle_T}{\langle I(q,t)\rangle_T^2} = 1 + c\,|f(q,\tau)|^2 \qquad (1)$$

was measured by dynamic light scattering (c = instrumental constant; $q = (4\pi n_D/\lambda)\sin\vartheta$; scattering angle $2\vartheta = 90°$; n_D = refractive index of dispersing medium; λ = wavelength of the laser light). The intermediate scattering function $f(q,\tau)$ was analyzed via the cumulant method [18], yielding the diffusion coefficient D_o and, via the Stokes-Einstein equation, $D_o = kT/6\pi\eta R_H$, the hydrodynamic radius $R_H = \langle R^6\rangle/\langle R^5\rangle$, where $\langle R^n\rangle$ denotes the n-th moment of the particle size distribution, k the Boltzmann constant, T the temperature and η the shear viscosity of the dispersing medium. From the position of the minimum of the particle form factor P(q), measured by static light scattering, the first moment of the particle size distribution $\langle R\rangle$ was derived according to

Ludwigshafen,Germany

$q\langle R\rangle$=4.49 [9,19]. For particle radii smaller than about 120 nm this procedure is inapplicable.

In order to determine the size polydispersity $\sigma = (\langle R^2\rangle - \langle R\rangle^2)^{1/2}/\langle R\rangle$ the full particle size distribution (PSD) was determined via various fractionation techniques (cf. Tab.1) and σ obtained by a gaussian fit of the PSD. Finally, the volume swelling ratio S was calculated from the particle radii in aqueous dispersion and in organic solvents, i.e. $S = R^3_{solv} / R^3_{aq.disp.}$. Tab.1 summarizes the characterization for the microgel particles used in this study.

2.4 Determination of the Static Structure Factor

In concentrated colloidal dispersions the time averaged intensity $\langle I(q)\rangle_T$ measured in an elastic (light or neutron) scattering experiment is given by [9]

$$\langle I(q)\rangle_T = N\, P(q)\, S(q)\,, \qquad (2)$$

where N denotes the number of colloidal particles, P(q) the particle form factor which contains information about particle size and shape, and S(q) the static structure which represents the structural arrangement of the particles. The latter and, thus, the static structure factor is determined by the particle interactions. Within the theory of simple liquids well developed techniques exist to calculate S(q) ab initio for a given interaction potential [20]. For the case of polydisperse hard spheres efficient algorithms are available that can be used to model S(q) of colloidal dispersions with hard sphere like interactions for various particle size distributions [21].

The extraction of S(q) from elastic scattering experiments on concentrated dispersions is achieved by dividing through the intensity $\langle I(q)\rangle_T$ measured in dilute dispersion, where S(q) = 1. This procedure requires that the particle form factor P(q) is independent of the concentration, a condition that is not necessarily fulfilled for more weakly crosslinked microgel particles. From previous SANS experiments we know that a change in P(q), corresponding to a size decrease, has to be taken into account above volume fractions of 0.5 for the 1:50 crosslinked PS microgel particles ADM18 [12]. However, it turned out that this had no significant effect on the extracted S(q) [16]. For higher crosslink densities (1:20) P(q) was independent of volume fraction. Thus the extraction of S(q) from elastic scattering data by dividing out P(q) could be savely performed for samples ADM18 (measured by SANS) as well as ADS257 (measured by light scattering).

Since similar results for the volume fraction dependence of the particle form factor were not available for crosslinked PTBA microgels, a different strategy was adopted to determine S(q) for the sample SK-25. Here, we used the fact that the apparent diffusion coefficient $D_{app}(q)$ obtained from the initial decay of the intermediate scattering function measured in DLS experiments is connected to the static structure factor via [9]

$$-q^{-2}\lim_{\tau\to 0}\frac{d}{d\tau}\ln f(q,\tau) = D_{app}(q) = D_o\frac{H(q)}{S(q)}\,. \qquad (3)$$

Here, H(q) is the hydrodynamic factor which accounts for the hydrodynamic interactions between colloidal particles in a homogeneous medium [9]. H(q) has been calculated for hard sphere colloids via many body hydrodynamic theory [22]. This allows to check if highly crosslinked microgel spheres can be treated as hard spheres. For this purpose we used the H(q) data from Ref.[22] to calculate experimental structure factors from the measured apparent diffusion coefficients $D_{app}(q)$ according to Eq.(3). These were then compared with theoretical structure factors for polydisperse hard spheres calculated according to Ref.[21]. For the light scattering experiments on concentrated dispersions isorefractive solvents (4-fluorotoluene for PTBA; 2-ethylnaphthlene for PS) were used to suppress multiple scattering. For the neutron scattering experiments on ADM18 deuterated toluene was used to minimize incoherent scattering.

3. Results and Discussion

Fig.2 compares the static structure factors of 1:10 crosslinked PTBA microgel spheres in the isorefractive solvent 4-fluorotoluene, obtained from DLS and using Eq.(3), with theoretical calculations for polydisperse hard spheres according to Ref.[21] for three volume fractions. Using the polydispersity σ = 0.04 as determined

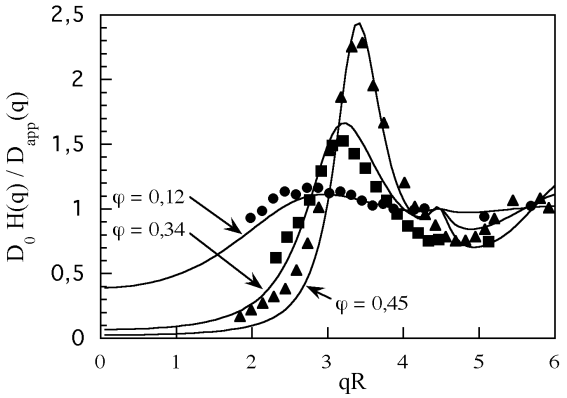

Fig.2 Comparison of the static structure factor S(q) of 1:10 crosslinked poly(t-butylacrylate) microgel particles in the good, isorefractive solvent 4-fluorotoluene with the theory for polydisperse hard spheres. The experimental S(q) (symbols) was determined from measurements of the apparent diffusion coefficient $D_{app}(q)$ by dynamic light scattering and literature data for the hydrodynamic factor H(q) (from Ref.[22]) according to $S(q) = D_o\, H(q)/\, D_{app}(q)$ (cf. Eq.3). Here, D_o denotes the free Stokes-Einstein diffusion coefficient. The theoretical S(q) (solid lines) were calculated using an algorithm developed by Vrij (Ref. [21]) using a hard sphere radius of R_{HS} = 255 nm and a size polydispersity of σ = 0.04. The volume fractions are φ = 0.12, φ = 0.34 and φ = 0.45 as indicated in the figure. The abszissa was rescaled using $R = R_{HS}$.

from the particle characterization the hard sphere radius R_{HS} is the only free parameter for matching the theory curves to the

experimental data. The best match was achieved with R_{HS} = 255 nm, a value slightly smaller (about 4%) than that obtained from particle characterization. As can be taken from the figure, the agreement is quite convincing, demonstrating that highly crosslinked microgel spheres can be considered to behave like hard sphere colloids. This view is supported by measurements of the long-time self diffusion coefficients [23] which agree quantitatively with theoretical predictions for hard sphere colloids from many-body hydrodynamics [24] up to a volume fraction of φ = 0.56.

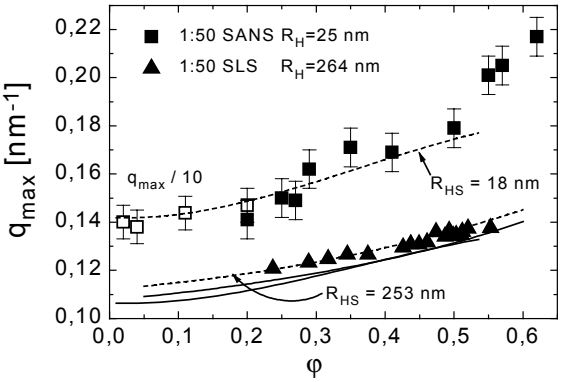

Fig.3 Volume fraction dependence of the position q_{max} of the main peak of the static structure factor S(q) for two 1:50 crosslinked polystyrene microgel spheres of different size (symbols) as compared to hard sphere theory [21] (lines). The experimental data were derived from elastic scattering experiments by dividing the time-averaged intensity measured for concentrated dispersions (cf. Eq.2) by the particle form factor measured in dilute dispersion (■: R_H = 25 nm, SANS in deuterated toluene; □: R_H = 25 nm, SAXS in deuterated toluene (taken from Ref.16); ▲ : R_H = 264 nm, static light scatterig in 2-ethylnaphthalene). The solid lines correspond to the theoretical peak positions calculated by use of the hydrodynamic radii R_H and the polydispersities as obtained from the particle characterization (cf. Tab.1). In order to match the theoretical peak positions to those observed in experiment effective hard sphere radii of R_{HS} = 18 nm and R_{HS}= 253 nm had to be used (dashed lines). Note that the the SANS and SAXS values for q_{max} were reduced by a factor of 10 for better comparison.

Figs.3 and 4 show the results for the 1:50 crosslinked microgel particles. Here, the data are reduced to the comparison of the position q_{max} and the height $S(q_{max})$ of the experimental static structure factor with hard sphere theory over the full volume fraction range up to φ = 0.62. Again the hard sphere radii had to be given smaller values as the determined particle sizes (the σ were again set to the values in Tab.1) in order to describe the φ-dependence of the peak positions of the experimental S(q) by hard sphere theory. This is demonstrated by the solid lines in Fig.3, which correspond to the peak positions calculated with the hydrodynamic radii from sample characterization. They systematically underestimate the experimental values. In case of the small ADM18 microgel particles this is a large effect. Adjusting the hard sphere radii to R_{HS} = 253 nm (4% smaller) and R_{HS} = 18 nm (about 30% smaller) for particles ADM18 and ADS257, respectively, theoretical and experimental peak positions coincide up to volume fractions of about φ = 0.5 (dashed lines). For the small particles one observes a stronger shift in the peak positions as compared to theory at higher volume fractions, even with the adjusted hard sphere radius. This is

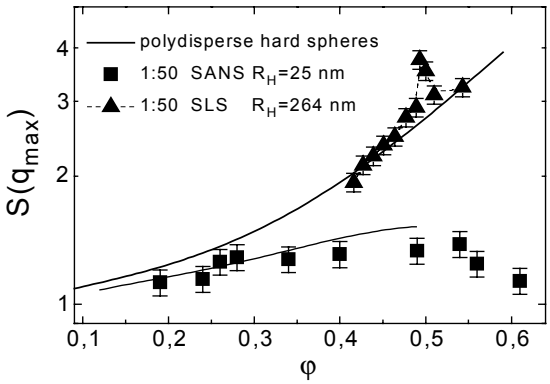

Fig.4 Volume fraction dependence of the height of the static structure factor peak $S(q_{max})$ for the 1:50 crosslinked microgel particles (symbols as in Fig.3) as compared to hard sphere theory (solid lines) using the effective hard sphere radii of Fig.3. Note that the absolute heights of the experimental data had to be matched to the theory (cf. Eq.2).

connected to the decrease in particle size that was previously observed with contrast variation SANS experiments [12].

Fig.4 compares the volume fraction dependence of the peak height $S(q_{max})$ of the different 1:50 crosslinked samples with hard sphere theory. The behaviour is quite different. The larger ADS257 particles follow hard sphere theory up to φ ≈ 0.47. Then they show a stronger increase followed by a sharp decrease of $S(q_{max})$ at φ >0.5. In contrast, the smaller ADM18 particles show a weaker increase of $S(q_{max})$ than hard sphere theory at volume fractions higher than about 0.4 and a decrease at φ >0.55.

From a comparison with analogous data for 1:10 crosslinked PS microgels, where hard sphere interactions are firmly established [25] and qualitatively similar behaviour was observed [26], we attribute the observation of a stronger increase of the experimental peak heights for ADS257 microgel particles to a failure of the theory. It is well known that the Percus Yevick approximation underlying the theoretical calculations becomes unreliable at high volume fractions [20]. Thus, the significant feature is the peak height decrease which indicates a loss of short range order. A similar behaviour has been observed for star polymers and has been interpreted as a change from predominantly colloidal behaviour to polymer-like behaviour due to the interpenetration of the particles when reaching the overlap concentration [27]. In analogy we interpret the peak height decrease as indication that the colloidal character of the particles becomes superposed by the internal gel character of the swollen polymer spheres leading to a significant deformation of the spheres and a concomitant loss of structural order at higher volume fractions. This interpretation is supported by the finding that the volume fraction where the loss of order becomes apparent correlates with the swelling ratio: the higher the swelling

ratio S, the earlier the breakdown of order occurs (cf. Tab.1). For ADS257 (S = 5.5) this occurs at φ = 0.5, for ADM18 (S = 4.4) at φ = 0.55 and for 1:10 crosslinked PS microgels (S= 2.2) at φ = 0.58 [26].

The other interesting result of this comparison is that while the large 1:50 crosslinked microgels behave like hard spheres until the colloidal character is lost, this is not the case for the smaller 1:50 crosslinked microgels. Here, the weaker increase of $S(q_{max})$ can be taken as indication that the interactions differ from the hard sphere potential. This result is consistent with a study of the volume fraction dependence of the collective diffusion coefficent, where a soft repulsive interaction potential was proposed for small ($R_H \approx 25$ nm) 1:20 and 1:50 crosslinked microgel colloids which becomes softer and longer ranged on decreasing the crosslink density [13]. This is most likely due to dangling polymer ends at the surface which play the same role for the interactions as the grafted polymer layer in sterically stabilized lyophobic colloids. The average length of the dangling ends can be set equal to the length of the polymer chains between crosslinks in first approximation, if a statistical distribution of crosslinks over the microgel particle is assumed. Thus the interaction range is expected to increase on decreasing the crosslink density. From the theory of steric stabilization it is known, that not the absolute length is the decisive quantity for the range of interactions, but rather the ratio of this length and the particle radius [28]. This ratio, which is included in Tab.1 as $\Delta R/ R_H$ in percent, changes an order of magnitude, from about 5% to about 50%, when going from the larger 1:50 crosslinked PS microgels (ADS257) to the small ones (ADM18). This explains why we observe hard sphere behaviour for one sample and soft repulsive interactions for another, even though the average stoichiometric crosslink density is identical.

These results imply that hard sphere behaviour can be achieved irrespective of the crosslink density as long as the length of the dangling polymer chains at the microgel surface is small with respect to the particle radius ($\Delta R/ R_H \leq 5\%$). The effective hard sphere radius R_{HS} is found to be smaller than the particle radius. For the large 1:50 crosslinked PS microgels (ADS257) this difference of about 12 nm corresponds within experimental accuracy to the calculated length of the dangling chains (≈ 12.5 nm cf. Tab.1). For the 1:10 crosslinked PTBA microgels R_{HS} is much smaller than expected on the basis of the stoichiometric crosslink density (⟨R - R_{HS} = 15 nm instead of 2.5 nm) Only part of this discrepancy can be attributed to experimental errors in the determination of ⟨R (estimated to be ≈ 3% or 7 nm [29]). A possible reason could be an inhomogeneous distribution of the crosslinker that leads to a lower effective crosslink density and, thus, to longer dangling ends, at the particle surface. Evidence for such an effect in PTBA microgels has been discussed elsewhere [2].

In summary, we find that the interactions between microgel particles in good solvents are determined by two quantities: the length of the dangling polymer ends relative to the particle radius, $\Delta R/ R_H$, acting as steric stabilization layer, sets the range of the repulsive interactions. Short dangling ends (1-5% of the particle radius) lead to hard sphere behaviour, whereas soft repulsive interactions are observed if the length of the polymer chains at the microgel surface amounts to 50% of the particle radius. The swelling ratio determines the degree to which microgel spheres are compressible or deformable at high volume fractions and thus controls the volume fraction where the gel character of the particles becomes apparent by deviations from colloidal behaviour. This compressibility may also be expected to determine the steepness of the short-range repulsive part of the interactions already at small volume fractions. Thus, the optimal strategy to design a dispersion of microgel particles that behave as hard sphere colloids up to very high volume fractions consists of using highly crosslinked particles (e.g. 1:10) with a size guaranteeing $\Delta R/ R_H \leq 0.05$ in a good solvent that is isorefractive to the polymer and minimizes the swelling ratio at the same time. Such a system is currently used for studies at the colloid glass transition.

Acknowledgements

The authors would like to thank W. Mächtle, BASF AG, for analyzing the sample ADM18 with the analytical centrifuge, V. Frenz, Clariant AG, for capillary hydrodynamic fractionation experiments on sample SK-25 and M. Stamm for providing access to the small angle Xray scattering instruments at the Max-Planck-Institut for Polymer Research, Mainz. Financial support of the Deutsche Forschungsgemeinschaft through the SFB262 is gratefully appreciated.

Literatur

[1] M. Antonietti, W. Bremser and M. Schmidt, Macromol. **23**, 3796 (1990)

[2] S. Kirsch, A. Doerk, E. Bartsch, H. Sillescu, K. Landfester, H.-W. Spiess, W. Maechtle, Macromolecules submitted.

[3] M.J. Murry, M.J. Snowden, Adv. Coll. Interf. Sci. **54**, 73, (1995)

[4] M.S. Wolfe, Polym. Mater. **61**, 398, (1989)

[5] G.E. Morris, B. Vincent, M.J. Snowden, J. Colloid Interf. Sci. **190**, 198 (1997)

[6] A. Loxley, B. Vincent, Coll. Polym. Sci. **275**, 1108 (1997)

[7] M. Antonietti, Angew. Chemie **100**, 1813, (1988)

[8] E. Bartsch, in S. Yip (Ed.), *Relaxation kinetics in supercooled liquids - mode coupling theory and its experimental tests,* Transp. Theory Stat Phys. **24**, 1125 (1995)

[9] P.N. Pusey, in *Liquids, Freezing and the Glass Transition*, edited by J. P.Hansen, D.Levesque and J. Zinn-Justin (North-Holland, Amsterdam, 1991), p.765

[10] E. Bartsch, V. Frenz, J. Baschnagel, W. Schärtl, H. Sillescu, J. Chem. Phys. **106**, 3743 (1997).

[11] W. van Megen, in S. Yip (Ed.), *Relaxation kinetics in supercooled liquids - mode coupling theory and its experimental tests,* Transp. Theory Stat. Phys. **24**, 1017 (1995)

[12] S. Stölken, E. Bartsch, H. Sillescu, P. Lindner, Prog. Colloid Polym. Sci. 98, 155 (1995).

[13] F. Renth, E. Bartsch, A. Kasper, S. Kirsch, S. Stölken, H. Sillescu, W. Köhler, R. Schäfer, Prog. Colloid Polym. Sci., **100**, 127 (1996).

[14] P.J. Flory, *Principles of Polymer Chemistry*, Cornell University Press, Ithaka, 1953

[15] A. Kotera, F. Furusawa, Y. Takeda, *Kolloidzeitschrift und Zeitschrift für Polymere* **239**, 677 (1970)

[16] S. Stölken, Ph.D. thesis, Mainz 1996.

[17] B.J. Berne, R. Pecora, *Dynamic light scattering*, Wiley, New York, 1976

[18] D.E. Koppel. J. Chem. Phys. **57**, 4814 (1972)

[19] P.N. Pusey, W. van Megen, J. Chem. Phys., **80 (8)**, 3513, (1984)

[20] J.P. Hansen and I.R. McDonald, *Theory of simple liquids*, 2nd. edn. (Academic Press, London, 1986)

[21] A. Vrij, J. Chem. Phys. **71**, 3267 (1979)

[22] C.W.J. Beenackker, P. Mazur, Physica A 126, 349 (1984)

[23] E. Bartsch, S. Kirsch, F. Renth, H. Sillescu, to be published

[24] M. Tokuyama, I. Oppenheim, Physica **A 216**, 85 (1995)

[25] S. Kirsch, Ph.D. thesis, Mainz 1996; the phase diagram was shown to be identical to that of hard sphere colloids

[26] C. Pies, E. Bartsch, unpublished

[27] D. Richter, O. Jucknischke, L. Willner, F.J. Fetters, M. Lin, J.S. Huang, J. Roovers, C. Toporoski, L.L Zhou, J. Phys. IV **C8** (France), 3 (1993)

[28] W.B. Russel, D.A. Saville, W.R. Schowalter, "Colloidal Dispersions", Cambridge University Press, Cambridge 1991

[29] For narrow size distributions $\langle R \approx R_H$ (see Ref.9). However, $\langle R$ can be determined with better accuracy from the position of the minimum of the particle form factor.